

## The effect of r-process enhancement in binary CEMP-s/r stars

---

**S. Bisterzo\***

*Dipartimento di Fisica Generale, Università di Torino, via P. Giuria 1, 10025 Torino, Italy*  
*E-mail: bisterzo@ph.unito.it*

**R. Gallino**

*Dipartimento di Fisica Generale, Università di Torino, via P. Giuria 1, 10025 Torino, Italy*  
*INAF Osservatorio Astronomico di Collurania, via M. Maggini, 64100 Teramo, Italy*  
*E-mail: gallino@ph.unito.it*

About half of carbon and *s*-process enhanced metal-poor stars (CEMP-*s*) show a high *r*-process enrichment (CEMP-*s/r*), incompatible with a pure *s*-process contribution. CEMP-*s* stars are of low mass ( $M < 0.9 M_{\odot}$ ) and belong to binary systems. The C and *s*-process enrichment results from mass transfer by the winds of the primary AGB companion (now a white dwarf). The nucleosynthesis of the *r*-process, instead, is believed to occur in massive stars exploding as Supernovae of Type II. The most representative *r*-process element is Eu (95% of solar Eu).

We suggest that the *r*-process enrichment was already present by local SNII pollution in the molecular cloud from which the binary system formed. The initial *r*-enrichment does not affect the *s*-process nucleosynthesis. However, the *s*-process indicators [hs/l<sub>s</sub>] (where l<sub>s</sub> is defined as the average of Y and Zr; hs as the average of La, Nd, Sm) and [Pb/hs] may depend on the initial *r*-enhancement. For instance, the hs-peak has to account of an *r*-process contribution estimated to be 30% for solar La, 40% for solar Nd, and 70% for solar Sm. A large spread of [Eu/Fe] is observed in unevolved halo stars up to [Eu/Fe]  $\sim 2$ . In presence of a very high initial *r*-enrichment of the molecular cloud, the maximum [hs/Fe] predicted in CEMP-*s/r* stars may increase up to 0.3 dex. Instead, the spread of [Y,Zr/Fe] observed in unevolved halo stars reaches a maximum of only  $\sim 0.5$  dex, not affecting much the predicted [l<sub>s</sub>/Fe]. This is in agreement with observations of CEMP-*s/r* stars that show an observed [hs/l<sub>s</sub>] in average higher than that observed in CEMP-*s*. Preliminary results are presented.

## 1. Introduction

It is commonly believed that the *s*- and *r*-processes derive from separate astrophysical sites [1]. The nucleosynthesis of the *s*-process occurs in stars of low mass ( $1.3 \leq M/M_{\odot} \leq 8$ ) during their thermally pulsing asymptotic giant branch (TP-AGB) phase. The main neutron source is the  $^{13}\text{C}(\alpha, n)^{16}\text{O}$ , which burns radiatively at  $T \sim 0.9 \times 10^8$  K during the interpulse period in the region between the H- and He-shell (He-intershell). A second neutron source,  $^{22}\text{Ne}(\alpha, n)^{25}\text{Mg}$ , is marginally activated at the bottom of the recurrent convective thermal instability (thermal pulse, TP) in the He-intershell, mainly affecting the abundance at the branching points that are sensitive to temperature and neutron density. The *s*-process elements are mixed with the surface during the third dredge-up (TDU) episodes, in which the convective envelope engulfs part of the He-intershell, after the quenching of a TP. We refer to the reviews by [2, 3] for major details on the AGB nucleosynthesis.

Instead, the physical environment for the *r*-process is still unknown, although SNII are the most promising candidates. For elements from Ba to Bi, observations of very metal-poor stars with high *r*-enhancement (e.g., CS 22892–052 [4]) show an abundance distribution well reproduced by a scaled solar *r*-process residual contribution [5]. Instead, lighter neutron capture elements with  $Z \leq 47$  show values lower than the scaled solar-system *r*-process [6, 7]. The nucleosynthesis site(s) and the exact contributions from different primary processes to Sr, Y, Zr is highly debated [8, 9, 10, 11, 12], although also related to massive stars. A large spread is observed for [Eu/Fe] and for [Sr,Y,Zr/Fe] in unevolved halo stars. For [Fe/H] < -2, different ranges are observed for Eu and Sr, Y, Zr:  $-1 \leq [\text{Eu}/\text{Fe}] \leq 2$  with an average around 0.5 dex, while  $-1 \leq [\text{Sr}, \text{Y}, \text{Zr}/\text{Fe}] \leq 0.5$  with an average around 0 dex [8, 12]. This may be interpreted as a signature of incomplete mixing in the gas cloud from which these stars have formed [13, 14], as well as an indication of different and uncorrelated primary process contributions.

In the last years, a quite large number of carbon and *s*-process enhanced metal-poor (CEMP-*s*) stars have been detected. CEMP-*s* are main-sequence/turnoff or giants of low mass ( $M < 0.9 M_{\odot}$ ). The most plausible explanation for their peculiar high *s*-element abundances is mass transfer by stellar winds from the most massive AGB companion (now a white dwarf). About half of these CEMP-*s* stars are also highly enhanced in *r*-process elements (CEMP-*s/r*). The observed *r*-enhancement in these stars reflects the observations of unevolved Galactic stars at low metallicity. CEMP-*s/r* stars show abundance patterns incompatible with a pure *s*-process nucleosynthesis. While a pure *s*-process predicts [La/Eu]  $\sim 0.8 - 1.1$  (where La and Eu are typical *s*- and *r*-process elements, respectively), CEMP-*s/r* stars show  $0.0 \leq [\text{La}/\text{Eu}] \leq 0.4$ , with [La/Fe] and [Eu/Fe] up to  $\sim 2$  dex. Different scenarios have been proposed in the literature to explain the origin of CEMP-*s/r* (e.g., [15, 16]).

We suggest that the molecular cloud from which the binary system formed was already enriched in *r*-process elements by local pollution of SNII ejecta [7, 18]. This hypothesis is supported by numerical simulations by [17], who found that SNII explosion in a molecular cloud may trigger the formation of binary systems. These simulations may explain the very high fraction of CEMP-*s/r* ( $\sim 50\%$ ) among the CEMP-*s*.

We present here a preliminary analysis of a comparison between AGB theoretical predictions and spectroscopic observations of CEMP-*s* and CEMP-*s/r* stars. A detailed discussion will be

presented in Bisterzo et al. (in preparation).

## 2. Results

Among CEMP-*s* stars in the literature, we selected only those with Eu detection. About half of them are CEMP-*s/r*.

In Fig. 1, we analyse the *s*-process indicator [hs/l<sub>s</sub>] (where l<sub>s</sub> = Y, Zr and h<sub>s</sub> = La, Nd, Sm) versus metallicity, by comparing CEMP-*s/r* and CEMP-*s* observations with AGB models of initial mass  $M = 1.3 M_{\odot}$  (left panel) or  $1.5 M_{\odot}$  (right panel). AGB models are described by [19] (updated by [20]). Starting from the case ‘ST’ defined by [19, 5], a range of <sup>13</sup>C-pockets is adopted by multiplying or dividing the <sup>13</sup>C (and <sup>14</sup>N) in the pocket by different factors. Theoretical lines in the Figure represent pure *s*-process AGB predictions for cases from ‘ST×2’ down to ‘ST/150’. For simplicity, in this preliminary analysis we distinguish between main-sequence/turnoff stars or subgiants having not suffered the first dredge-up (FDU) episode (diamonds in left panel), and late subgiants or giants (down-rotated triangles in right panel). The FDU involves about 80% of the mass of the star [2]. In case of binary systems with mass transfer like CEMP-*s* stars, this mixing strongly dilutes the C and *s*-rich material previously transferred from the AGB companion. This means that the [Ei/Fe] observed in a CEMP-*s* giant is about 1 dex lower than in the envelope of the AGB companion<sup>1</sup>. CEMP-*s/r* stars are represented by big symbols while CEMP-*s* by little symbols. References are given in the caption of the Figures. In average, CEMP-*s/r* stars show higher [hs/l<sub>s</sub>] than CEMP-*s*. Moreover, some CEMP-*s/r* have an observed [hs/l<sub>s</sub>] ratio higher than the AGB predictions, but still compatible within the errorbars.

In Fig. 2, the observed [hs/l<sub>s</sub>] ratio is compared with AGB models of initial masses  $M = 1.3 M_{\odot}$  (left panel) or  $1.5 M_{\odot}$  (right panel) with a high initial *r*-process enhancement,  $[r/Fe]^{\text{ini}} = 2.0$  dex (corresponding to  $[Eu/Fe]^{\text{ini}} = 2.0$  dex). Only CEMP-*s/r* stars are shown in this Figure (big symbols). The choice of the initial *r*-process contribution to heavy elements was based on the *r*-process solar predictions [5, 20]. In particular, we applied an initial *r*-process contribution of 30% to solar La, 40% to solar Nd, and 70% to solar Sm. In first approximation we assumed a solar-scaled Y and Zr. This because the [Y,Zr/Fe] ratios observed in unevolved halo stars reach maximum values of about 0.5 dex, which little affects the [l<sub>s</sub>/Fe] in CEMP-*s*. The resulting maximum [hs/l<sub>s</sub>]<sub>s+r</sub> with  $[r/Fe]^{\text{ini}} = 2.0$  shown in Fig. 2 is about 0.3 dex higher than the predicted [hs/l<sub>s</sub>]<sub>s</sub> with no initial *r*-enhancement. Note that the *s*-process index [hs/l<sub>s</sub>]<sub>s</sub> is independent of the dilution factor if no initial *r*-enhancement is adopted (Fig. 1, right panel). Instead, in case of a high initial *r*-enhancement, the dilution factor affects [hs/l<sub>s</sub>]<sub>s+r</sub>, because both stars belonging to the binary system are initially *r*-enriched. In Fig. 2, right panel, a dil = 1.0 dex is applied.

## 3. Conclusions

To explain the origin of CEMP-*s/r*, we hypothesised that the molecular cloud from which the binary system formed was already enriched in *r*-process elements. Subsequently, the *s*-process

<sup>1</sup>To simulate mixing processes we define the logarithmic ratio ‘dil’ as  $\text{dil} = \log\left(\frac{M_{\star}^{\text{env}}}{\Delta M_{\text{AGB}}^{\text{trans}}}\right)$ , where  $M_{\star}^{\text{env}}$  represents the mass of the convective envelope of the observed star before the mixing, and  $\Delta M_{\text{AGB}}^{\text{trans}}$  is the AGB total mass transferred (see [20]).

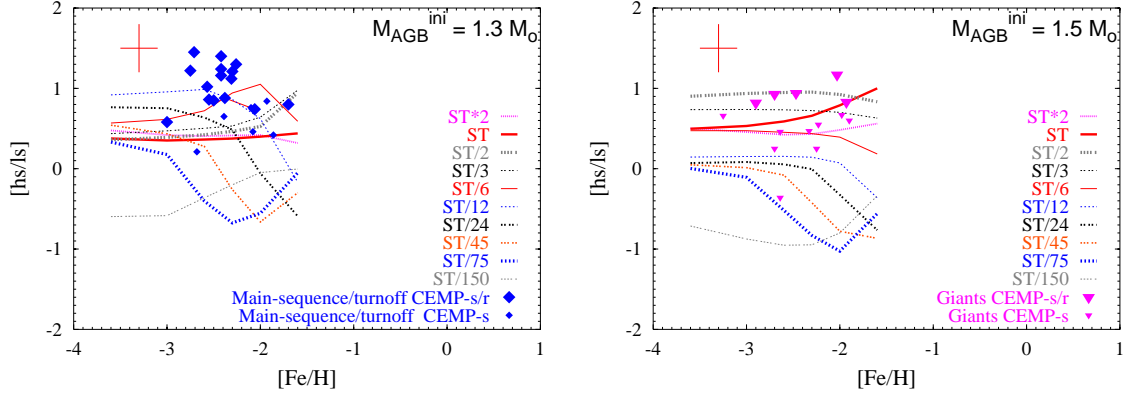


**Figure 1:** Left panel: the [hs/ls] ratios observed in main-sequence/turnoff or subgiants CEMP-*s* and CEMP-*s/r* stars versus metallicity, compared with AGB models of initial mass  $M = 1.3 M_{\odot}$  and a range of  $^{13}\text{C}$ -pockets. References are [21, 22, 23, 24, 25, 16, 26, 27, 28, 29, 15, 30, 31]. Right panel: the [hs/ls] ratios observed in CEMP-*s* and CEMP-*s/r* giants versus metallicity, compared with AGB models of initial mass  $M = 1.5 M_{\odot}$  and a range of  $^{13}\text{C}$ -pockets. Similar predictions are obtained by  $M = 2 M_{\odot}$  models. References are [32, 22, 33, 24, 26, 34, 35, 36, 37, 38]. No initial *r*-process enhancement is assumed in both cases.

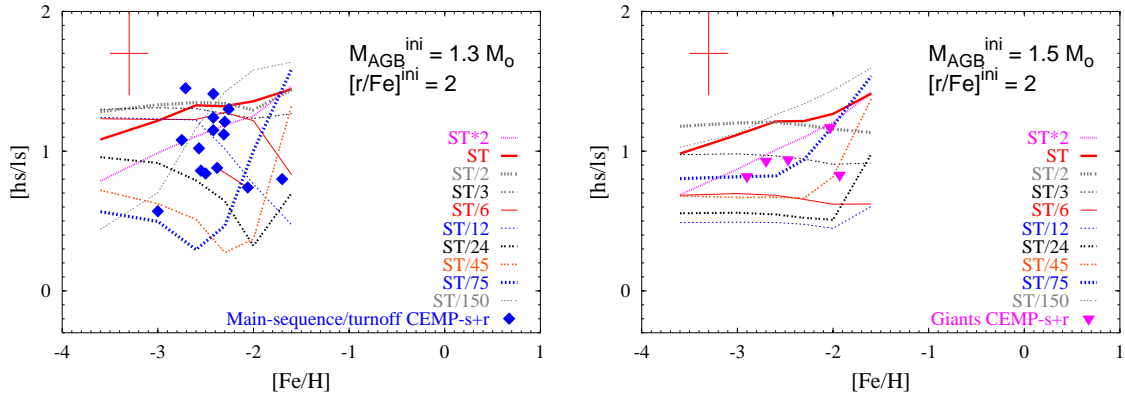


**Figure 2:** Left panel: the [hs/ls] ratios observed in main-sequence/turnoff or subgiant CEMP-*s/r* stars versus metallicity, compared with AGB models of initial mass  $M = 1.3 M_{\odot}$  and a range of  $^{13}\text{C}$ -pockets. Right panel: the [hs/ls] ratios observed in CEMP-*s/r* giants versus metallicity, compared with AGB models of initial mass  $M = 1.5 M_{\odot}$  and a range of  $^{13}\text{C}$ -pockets. An initial *r*-enhancement of  $[r/\text{Fe}]^{\text{ini}} = 2.0$  dex is adopted in both cases. A dilution of 1 dex is applied to  $M = 1.5 M_{\odot}$  models, which best accounts for giant CEMP-*s* or CEMP-*s/r*.

elements synthesised by the AGB companion are transferred by stellar winds on to the observed star. The *s*-process nucleosynthesis is not affected by the initial *r*-enhancement of the molecular cloud. However, for high *r*-process enrichment ( $[r/\text{Fe}]^{\text{ini}} = 2$ ), one should account for the *r*-process contribution to solar La, Nd and Sm (30%, 40%, 70%). In agreement with the [Y,Zr/Fe] observed in unevolved halo stars, we adopt solar scaled initial Y and Zr values. This increases [hs/ls] by  $\sim 0.3$  dex. This is sustained by observations in CEMP-*s/r* stars, which show an [hs/ls] ratio in average higher than that observed in CEMP-*s*. Note that the [hs/ls] observed in CEMP-*s/r* stars may be in agreement with pure *s*-process predictions within the errorbars. A deeper analysis will be given in Bisterzo et al., in preparation.

## References

- [1] Burbidge, E. M., Burbidge, G. R., Fowler, W. A. Hoyle, F. 1957, *Rev. Mod. Phys.*, 29, 4
- [2] Busso, M., Gallino, R. & Wasserburg, G. J., 1999, *ARA&A*, 37, 239
- [3] Käppeler, F., et al., 2010, *Rev. Mod. Phys.*, accepted
- [4] Sneden, C., et al. 2003, *ApJ*, 591, 936
- [5] Arlandini et al. (1999), *ApJ*, 525, 886
- [6] Wasserburg, G. J., Busso, M. & Gallino, R. 1996, *ApJ*, 466, L109
- [7] Sneden, C., Cowan, J. J., Gallino, R. (2008), *ARA&A*, 46, 241
- [8] Travaglio et al. 2004, *ApJ*, 601, 864
- [9] Farouqi, K., et al. 2010, *ApJ*, 712, 1359
- [10] Pignatari, M. et al. 2010, *ApJ*, 710, 1557
- [11] Qian, Y.-Z. & Wasserburg, G.J. 2008, *ApJ*, 687, 272
- [12] Montes, F., et al. 2007, *ApJ*, 671, 1685
- [13] Ishimaru, Y., & Wanajo, S. 1999, *ApJ*, 511, L33
- [14] Travaglio, C., Galli, D., & Burkert, A. 2001, *ApJ*, 547, 217
- [15] Jonsell et al. (2006), *A&A*, 451, 651
- [16] Cohen et al. (2003), *ApJ*, 588, 1082
- [17] Vanhala & Cameron (1998), *ApJ*, 508, 291
- [18] Bisterzo et al. (2009), *PASA*, 26, 314
- [19] Gallino et al. (1998), *ApJ*, 497, 388
- [20] Bisterzo et al. (2010), *MNRAS*, 404, 1529
- [21] Aoki, W., et al. 2002b, *ApJ*, 580, 1149
- [22] Aoki, W., et al. 2006, *ApJ*, 650, 127
- [23] Aoki, W. et al. 2008, *ApJ*, 678, 1351
- [24] Barklem, P. S. et al. 2005, *A&A*, 439, 129
- [25] Behara, N. T., et al. 2010, *A&A*, 513, A72
- [26] Cohen, J. G. et al. 2006, *AJ*, 132, 137
- [27] Ivans et al. (2005), *ApJ*, 627, 145
- [28] Johnson, J. A., & Bolte, M. 2002, *ApJ*, 579, 87
- [29] Johnson, J. A., & Bolte, M. 2004, *ApJ*, 605, 462
- [30] Thompson, I. B. et al. 2008, *ApJ*, 677, 556
- [31] Tsangarides, S. A. 2005, Ph.D. Thesis, Open University (United Kingdom), DAI-C 66/04
- [32] Aoki, W. et al. 2002a, *PASJ*, 54, 427
- [33] Barbuy, B., et al. 2005, *A&A*, 429, 1031
- [34] Goswami, A., & Aoki, W. 2010, *MNRAS*, 404, 253
- [35] Goswami, A., et al. 2006, *MNRAS*, 372, 343
- [36] Masseron, T. et al. 2006, *A&A*, 455, 1059
- [37] Roederer, I. U. et al. 2008, *ApJ*, 679, 1549
- [38] Van Eck, S., Goriely, S., Jorissen, A., Plez, B. 2003, *A&A*, 404, 291